

Optical second harmonic generation from low-lying excited states in potassium vapour

This content has been downloaded from IOPscience. Please scroll down to see the full text.

1990 J. Phys. B: At. Mol. Opt. Phys. 23 921

(<http://iopscience.iop.org/0953-4075/23/5/014>)

View [the table of contents for this issue](#), or go to the [journal homepage](#) for more

Download details:

IP Address: 140.113.38.11

This content was downloaded on 28/04/2014 at 19:50

Please note that [terms and conditions apply](#).

Optical second harmonic generation from low-lying excited states in potassium vapour

Mao-hong Lu and Juin-huei Tsai

Institute of Electro-optical Engineering, National Chiao-Tung University, Hsinchu, Taiwan 30050, Republic of China

Received 24 October 1989

Abstract. Optical second harmonic generation has been observed on or near the $4s^2S_{1/2}-6s^2S_{1/2}$, $4s^2S_{1/2}-np^2P_{1/2,3/2}$ ($n = 5, 6$) and $4s^2S_{1/2}-nd^2D_{5/2,3/2}$ ($n = 3, 4$) two-photon resonances in potassium vapour, as laser scanning in the 660-940 nm wavelength range. The second harmonic intensities and ionisation currents have been measured as a function of pumping laser detuning from the two-photon resonances. On or near the two-photon resonances, the intensity and vapour-density dependence of second harmonic generation have also been investigated. The saturation of second harmonic generation has been observed. Some calculations and analyses have been made with the $\chi^{(3)}$ model. The results have been compared with the measurements. Based on these analyses, the mechanisms for second harmonic generation in isotropic vapours are discussed.

1. Introduction

Optical second harmonic generation (SHG) in isotropic vapours is of great interest theoretically and experimentally because it is strictly forbidden by symmetry under the electric dipole approximation. In the last ten years many experiments on SHG in several metal vapours have been reported. Two mechanisms were put forward to explain the SHG in the isotropic vapours. One (Mossberg *et al* 1978, Okada *et al* 1981, Bethune 1981) attributes the SHG to the contribution of the third order susceptibility $\chi^{(3)}$, where a laser-induced static electric field is involved. The other (Dinev *et al* 1983) attributes the SHG to collisional l mixing of states. Recently Elci *et al* (1988) proposed a theory to explain the SHG with collision complexes. However, according to Gallagher *et al* (1977), the collisional l mixing only occurs for highly excited states with $l \geq 2$. They found that the sodium d states with the principal quantum number $n \geq 5$ were mixed with the nearly degenerate higher l states of the same n , but the s and p states did not exhibit this effect. If the collisional l mixing mechanism is responsible for the SHG by two-photon excitations of ns or nd states, the ns or nd state should be mixed with some p states. However, for low-lying excited s (or d) states, this is energetically difficult because the energy gap between p states and the s (or d) state is much larger than thermal energy. Therefore, it is interesting to observe the SHG from low-lying excited states.

More recently, the SHG in potassium vapour by two-photon resonances of high-lying s, p, and d states ($n = 7-34$) was measured by Dinev (1988a, b). The SHG in potassium vapour from ns 2S ($n = 7-9$), np 2P ($n = 7, 8$), and nd 2D ($n = 5-7$) states by two-photon resonances was also measured by Lu *et al* (1989). In this paper, we present some new

results on SHG from the ns^2S ($n=6$), np^2P ($n=5, 6$), and nd^2D ($n=3, 4$) low-lying states in potassium vapour. The conversion efficiencies of SHG on the two-photon resonances have been evaluated. We measured the SH intensities and ionisation currents as a function of pumping laser detuning from the two-photon resonances. We also measured the intensity dependence and the vapour-density dependence of SHG on or near the two-photon resonances. A strong saturation in the intensity dependence of SHG has been observed. Some calculations and analyses have been made with the $\chi^{(3)}$ model to explain the observed results. Based on these analyses, the mechanisms for SHG in isotropic vapours are discussed.

2. Experiment

The apparatus is shown schematically in figure 1. A tunable pulsed dye laser (Quanta-Ray, PDL-1) pumped by a frequency-doubled $Nd^{3+} : YAG$ laser was used as light source. Typical operating parameters for the dye laser were: 20 ns pulse duration, 3–5 mJ pulse energy, 0.2 cm^{-1} linewidth and 10 Hz repetition rate. The dyes LDS 698, 751, 821, and 867 (Exciton Inc) were used to cover the wavelength ranges 658–738, 714–792, 785–851 and 840–940 nm, respectively. According to the energy level diagram of potassium, shown in figure 2, the dye-laser scanning in these wavelength ranges can reach the two-photon resonances of the $6s^2S$, $5p^2P$, $6p^2P$, $3d^2D$ and $4d^2D$ states of potassium. In this experiment, the pumping waves were linearly polarised.

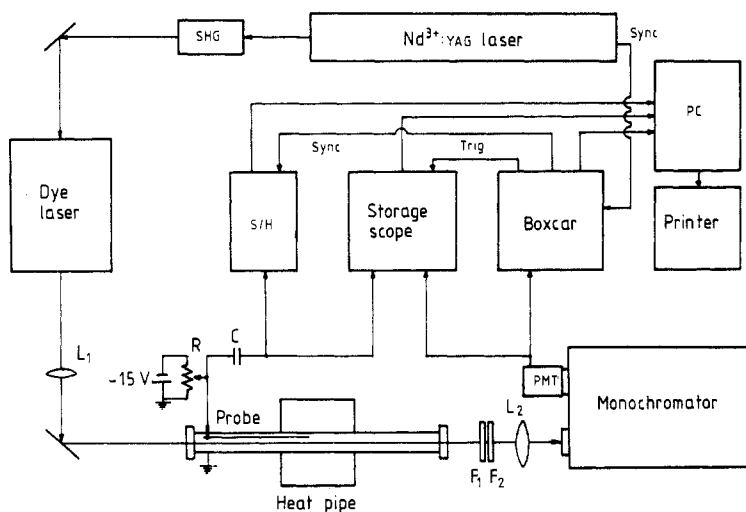


Figure 1. Experimental set-up.

Potassium vapour was enclosed in a heat pipe (Vidal and Cooper 1969) and heated to temperatures of 300–350 °C with a 30 cm heated zone. The vapour density was about 10^{14} – 10^{16} cm^{-3} . Argon gas at one mbar was used as a buffer gas. The laser beam was focused by an 80 cm focal length lens to a spot with a diameter of 0.25 mm at the centre of the heat pipe. The output radiation was first filtered against the strong pumping light and some parametric emissions with a combination of two filters (Melles Griot, UG11 and BG3 or UG11 and BG23), and then detected by a photomultiplier

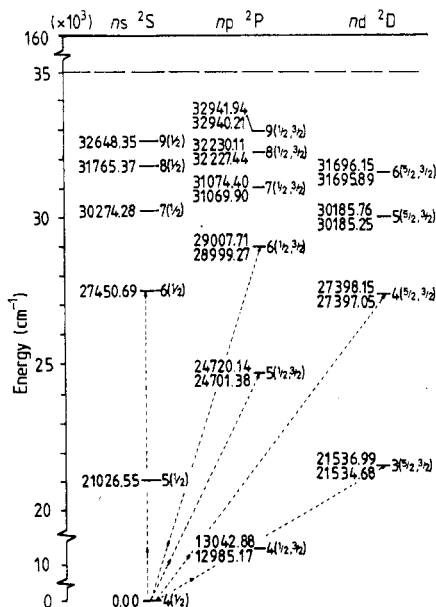


Figure 2. Energy level diagram of potassium.

tube in (PMT) (Hamamasu 1P28A and R928) after a 1 m monochromator (Spex 1704) with 50 μm entrance and exit slits. The wavelength accuracy measured in this experiment is about 0.04 nm. The monochromator was calibrated by the emission lines of a Cd-Hg lamp and a He-Ne laser. The signal from the PMT was fed into a boxcar (NF BX531). All the data were stored in a microcomputer and processed. The spectral response of the measurement system was corrected.

A stainless steel wire of about 2 mm diameter was used as a probe, to measure the ionisation current. A potential of -15 V was applied to the probe relative to the heat pipe wall during the ionisation current measurement. The signal from the probe was transferred to a microcomputer through a sample-and-hold (s/H).

3. Results and discussion

3.1. SHG on the two-photon resonances

When the laser wavelength was tuned to the $4s^2S-6s^2S$, $4s^2S-np^2P$ ($n=5, 6$), and $4s^2S-nd^2D$ ($n=3, 4$) two-photon resonances, we measured the SH spectral lines, as shown in figure 3. It is found that the SH intensities on these two-photon resonances are quite different. In order to explain these large differences, we use the four wave mixing model, i.e. $\chi^{(3)}$ model to calculate the ratios of the SH intensities. According to this model, assuming the fundamental field to be undepleted over the interaction length, indeed often in practice, the SHG in the plane-wave approximation can be expressed (Hanna *et al* 1979) as

$$I_2 = \frac{(2\omega)^2}{16\epsilon_0^2 c^4 n_1^2 n_0 n_2} |\chi^{(3)}(-2\omega; 0, \omega, \omega)|^2 I_1^2 I_0 L^2 \text{sinc}^2\left(\frac{\Delta k L}{2}\right) \quad (1)$$

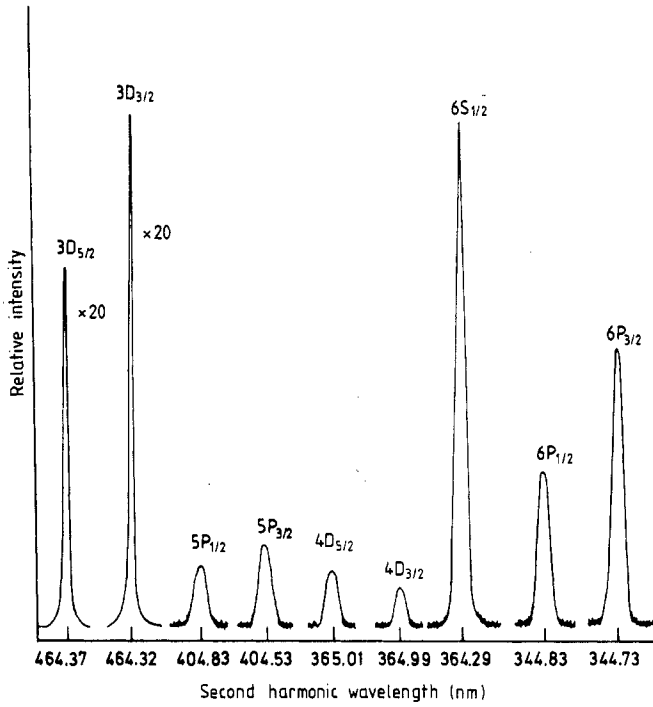


Figure 3. Spectra of SH radiation at the laser wavelengths tuned to the $4s^2S-n d^2D$ ($n = 3, 4$), $4s^2S-n p^2P$ ($n = 5, 6$) and $4s^2S-6s^2S$ two-photon resonances.

where I_2 , I_1 and I_0 are the intensities of SH, fundamental wave and laser-induced DC electric field, respectively, n_2 , n_1 , and n_0 are the refractive indices for these three fields, ω is the fundamental angular frequency, L is the interaction length, $\Delta k = k_2 - 2k_1$ is the phase mismatch and $\chi^{(3)}(-2\omega; 0, \omega, \omega)$ is the third-order susceptibility. For two-photon resonance, the $\chi^{(3)}$ is given by

$$\chi^{(3)}(-2\omega; 0, \omega, \omega) = \frac{1}{3} \frac{\bar{N}e^4}{\epsilon_0 h^3} \frac{1}{\Delta - i\Gamma} \sum_{a,b} \left[\frac{\langle g|z|a\rangle\langle a|z|f\rangle\langle f|z|b\rangle\langle b|z|g\rangle}{(\Omega_{ag} - 2\bar{\omega})(\Omega_{bg} - \bar{\omega})} + \frac{\langle g|z|a\rangle\langle a|z|f\rangle\langle f|z|b\rangle\langle b|z|g\rangle}{\Omega_{ag}(\Omega_{bg} - \bar{\omega})} \right] \quad (2)$$

where the $|a\rangle$ and $|b\rangle$ states must be p levels ($l = 1$) in this case as intermediate states, the $|g\rangle$ and $|f\rangle$ states are the ground state and the two-photon excited state, respectively, Ω_{ij} are the atomic transition frequencies in wavenumber and $\bar{\omega} = \omega/2\pi c$, $\Delta - i\Gamma$ is the resonant denominator in which $\Delta = 0$ on exact two-photon resonances, and Γ is a damping parameter, \bar{N} is equal to $N[\rho(g) - \rho(f)]$ representing the population difference of the transition where N is the density of atoms and $\rho(j)$ is the probability for an atom in the j state. In equation (2) we assume all the electric fields to be linearly polarised in the z direction. But this assumption is not true for the SH and DC fields. Actually, the DC field (Bethune 1981) and some SH fields (Dinev 1988a) are not polarised in the z direction. This assumption is only for simplifying the calculation. For a focused laser beam, if the confocal parameter is much greater than the interaction

length, as in our case, the plane-wave approximation is a good approximation. We follow the procedure of Eicher (1975) to calculate $\chi^{(3)}$ using equation (2) for the $4s^2S_{1/2}-nd^2D_{3/2,5/2}$ ($n=3, 4$), $4s^2S_{1/2}-np^2P_{1/2,3/2}$ ($n=5, 6$), and $4s^2S_{1/2}-6s^2S_{1/2}$ two-photon resonances. In this calculation, the oscillator strengths $f(n, l \rightarrow n', l+1)$ are taken from Lindgared and Nielsen (1977) and the energy levels are taken from Bashkin and Stoner (1975). The calculated results are listed in table 1. The ratio of the SH intensities produced by the different two-photon resonances, a and b , can approximately be evaluated from equations (1) and (2):

$$\frac{I_2(a)}{I_2(b)} \approx \left(\frac{\omega_a}{\omega_b}\right)^2 \left|\frac{\chi_a^{(3)}}{\chi_b^{(3)}}\right|^2 \left(\frac{I_0(a)}{I_0(b)}\right) \quad (3)$$

here, for simplicity, the phase mismatch factors in (2) are assumed to be equivalent for both the two-photon resonances.

Table 1. The calculated third-order susceptibilities (m V^{-1}) and measured conversion efficiencies for SHG. The ground state is $4s^2S_{1/2}$.

Upper states	$ \chi^{(3)} (\Gamma/\bar{N})^\dagger$ ($\times 10^{-33}$)	Conversion efficiency ($\times 10^{-7}$)
$3d^2D_{5/2}$	8.3	43
$3d^2D_{3/2}$	5.5	61
$5p^2P_{1/2}$	13.4	0.35
$5p^2P_{3/2}$	16.6	0.53
$4d^2D_{5/2}$	0.73	0.29
$4d^2D_{3/2}$	0.49	0.21
$6s^2S_{1/2}$	7.6	2.6
$6p^2P_{1/2}$	0.54	0.80
$6p^2P_{3/2}$	1.01	1.4

$\dagger \Gamma$ is a damping parameter and \bar{N} is ($N_g - N_f$) representing the population difference between the ground state and the upper state.

For the $4s^2S_{1/2}-3d^2D_{5/2}$ and $4s^2S_{1/2}-4d^2D_{5/2}$ two-photon resonances, the ratio of SH intensities is

$$\frac{I_2(4S-3D_{5/2})}{I_2(4S-4D_{5/2})} = 78.9 \times \left[\frac{\bar{N}(4S-3D_{5/2})\Gamma_{4D_{5/2}}}{\bar{N}(4S-4D_{5/2})\Gamma_{3D_{5/2}}} \right]^2 \left[\frac{I_0(4S-3D_{5/2})}{I_0(4S-4D_{5/2})} \right]. \quad (4)$$

If the terms in the square brackets are assumed to be one, the ratio is about 79 compared with the measured value 120, see figure 3. Considering so many approximations made above, the agreement between the calculated and the measured values is not bad.

Similarly, according to table 1, the $|\chi^{(3)}|$ is $8.3(\bar{N}/\Gamma) \times 10^{-33}$ for the $4s^2S_{1/2}-3d^2D_{5/2}$ two-photon resonance and $7.6(\bar{N}/\Gamma) \times 10^{-33}$ for the $4s^2S_{1/2}-6s^2S_{1/2}$ two-photon resonance. We take $\Gamma^{-1} = c\tau_{3d} = 1.24 \times 10^3 \text{ cm}$ for the $3d^2D_{5/2}$ and $\Gamma^{-1} = c\tau_{6s} = 2.63 \times 10^3 \text{ cm}$ for the $6s^2S_{1/2}$, where c is the velocity of light and τ_{3d} and τ_{6s} are the lifetimes of the $3d^2D$ and $6s^2S$ states respectively (Lindgared and Nielsen 1977), we have $|\chi^{(3)}| = 1.0 \times 10^{-37} [\bar{N}(4S-3D_{5/2})]$ for the $4s^2S_{1/2}-3d^2D_{5/2}$ two-photon resonance and $|\chi^{(3)}| = 2.0 \times 10^{-37} [\bar{N}(4S-6S)]$ for the $4s^2S_{1/2}-6s^2S_{1/2}$ two-photon resonance. With equation (3), the ratio of the SH intensities for both the two-photon resonances is given by

$$\frac{I_2(4S-3D_{5/2})}{I_2(4S-6S_{1/2})} = 0.15 \times \left[\frac{\bar{N}(4S-3D_{5/2})}{\bar{N}(4S-6S_{1/2})} \right]^2 \left[\frac{I_0(4S-3D_{5/2})}{I_0(4S-6S_{1/2})} \right]. \quad (5)$$

If the population difference \bar{N} and laser induced DC field were the same in both cases, the SH intensity from the $4s^2S_{1/2}$ - $6s^2S_{1/2}$ two-photon resonance would be larger than that from the $4s^2S_{1/2}$ - $3d^2D_{5/2}$ two-photon resonance. In fact, the measurement shows that the SH intensity from the $4s^2S_{1/2}$ - $3d^2D_{5/2}$ two-photon resonance is one order of magnitude larger than that from the $4s^2S_{1/2}$ - $6s^2S_{1/2}$ resonance (see figure 3). In order to understand this result, we measured the peak value of ionisation current at each step of laser scanning, as shown in figure 4. We found that the measured ionisation current for the $4s^2S$ - $6s^2S$ two-photon resonance was almost twice as large as that for the $4s^2S$ - $3d^2D$ two-photon resonance. As expected, the ionisation cross section should be much larger on the $4s^2S$ - $6s^2S$ two-photon resonance than on the $4s^2S$ - $3d^2D$ two-photon resonance because the former is due to three-photon ionisation, but the latter is due to four-photon ionisation. The ionisation reduces the population of the ground state much more severely on the $4s^2S$ - $6s^2S$ two-photon resonance than on the $4s^2S$ - $3d^2D$ two-photon resonance. The population reduction of the ground state causes the reduction of $\chi^{(3)}$, which is proportional to the population difference, i.e., the reduction of SH intensity in the $\chi^{(3)}$ model. That is why the SH intensity is much smaller on the $4s^2S$ - $6s^2S$ two-photon resonance than on the $4s^2S$ - $3d^2D$ two-photon resonance. Although more ionisation can produce a larger laser-induced DC field, which contributes to SHG, the effect of the population reduction of the ground state is considered to be predominant.

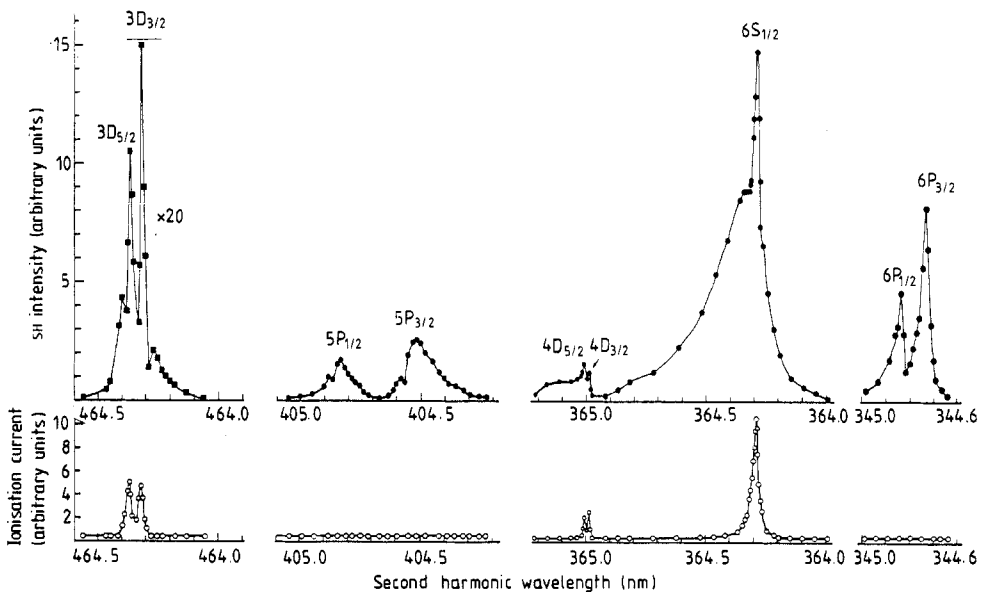


Figure 4. SH intensities and corresponding ionisation currents as a function of laser detuning from the $4s^2S$ - nd^2D ($n = 3, 4$), $4s^2S$ - np^2P ($n = 5, 6$), and $4s^2S$ - $6s^2S$ two-photon resonances. Here the potassium vapour density is $N_0 = 1.4 \times 10^{15} \text{ cm}^{-3}$ and the laser power intensity is $I_1 = 1.7 \times 10^8 \text{ W cm}^{-2}$.

The effect of ionisation on SHG is even clearer if we look at the fine structures for the $4s^2S$ - $3d^2D$ and $4s^2S$ - $4d^2D$ two-photon resonances in figure 4. We find that the $4s^2S_{1/2}$ - $3d^2D_{5/2}$ two-photon resonance, compared with the $4s^2S_{1/2}$ - $3d^2D_{3/2}$ two-photon resonance, relates to a larger ionisation current, but a smaller SH intensity. For

the $4s^2S_{1/2}-4d^2D_{3/2}$ and $4s^2S_{1/2}-4d^2D_{5/2}$ two-photon resonances, however, the $4s^2S_{1/2}-4d^2D_{3/2}$ two-photon resonance, compared with the $4s^2S_{1/2}-4d^2D_{5/2}$ two-photon resonance, corresponds to a smaller ionisation current, but a larger SH intensity.

From table 1 we find that the ratio of the $\chi^{(3)}$ ($4s^2S_{1/2}-5p^2P_{3/2}$) to the $\chi^{(3)}$ ($4s^2S_{1/2}-6p^2P_{3/2}$) is 16.4 ($\Gamma_{6p}/\Gamma_{5p} \approx 16.4$ ($\tau_{5p}/\tau_{6p} = 6.6$, where $\tau_{5p} = 121$ ns and $\tau_{6p} = 299$ ns are the lifetimes of the $5p^2P$ and $6p^2P$ states respectively, taken from Lindgard and Nielsen (1977), and the \bar{N} in both cases are assumed to be equivalent because the measured ionisation currents are almost the same, as shown in figure 4. The larger value of $\chi^{(3)}$ for the $4s^2S_{1/2}-5p^2P_{3/2}$ two-photon resonance, compared with the $\chi^{(3)}$ for the $4s^2S_{1/2}-6p^2P_{3/2}$, is due to the near-resonant enhancement by the $4p^2P$ level, of which the energy difference from the single photon is only about -625 cm^{-1} . From equation (3), we have

$$\frac{I_2(4S-5P_{3/2})}{I_2(4S-6P_{3/2})} \approx \frac{[\omega^2|\chi^{(3)}|^2I_0]_{4S-5P}}{[\omega^2|\chi^{(3)}|^2I_0]_{4S-6P}} = 30.4 \left[\frac{I_0(4S-5P_{3/2})}{I_0(4S-6P_{3/2})} \right]. \quad (6)$$

If we ignore the I_0 terms in equation (6), the SH intensity on the $4s^2S_{1/2}-5p^2P_{3/2}$ two-photon resonance should be more than one order of magnitude larger than that on the $4s^2S_{1/2}-6p^2P_{3/2}$ two-photon resonance. The measurement, however, shows that the SH intensity on the $4s^2S_{1/2}-5p^2P_{3/2}$ resonance is smaller than that on the $4s^2S_{1/2}-6p^2P_{3/2}$ resonance, as shown in figure 4. In order to explain this result, we consider the effect of the laser-induced DC field in (6). In the $\chi^{(3)}$ model this DC field, produced by multiphoton ionisation and free-electron expansion, is proportional to the square of the electron velocity (Okada *et al* 1981 and Bethune 1981), i.e., the kinetic energy of the electron after ionisation, which can be calculated as the energy difference between the three photons which induce the ionisation and the ionisation limit of potassium (Bashkin *et al* 1975). In equation (6), the ratio of the DC electric fields equals to the ratio of the electron kinetic energies \mathcal{E}_k corresponding to the $4s^2S_{1/2}-5p^2P_{3/2}$ and $4s^2S_{1/2}-6p^2P_{3/2}$ two-photon resonance ionisations. In addition, equation (6) has to be corrected by considering the single-photon absorption of the generated wave, which can make the $4s^2S_{1/2}-np^2P_{3/2}$ ($n = 5, 6$) one-photon transition. The SH intensity is inversely proportional to $\sigma^{(1)}$ (see equation (32)), i.e., $f(4s^2S_{1/2}-np^2P_{3/2})$, where $\sigma^{(1)}$ is the one-photon absorption cross-section and $f(4s^2S_{1/2}-np^2P_{3/2})$ is the absorption oscillator strength for the $4s^2S_{1/2}-np^2P_{3/2}$ transition, taken from Lindgard and Nielsen (1977). So we have

$$\begin{aligned} \frac{I_2(4S-5P_{3/2})}{I_2(4S-6P_{3/2})} &\approx 30.4 \left[\frac{\mathcal{E}_k(4S-5P_{3/2})}{\mathcal{E}_k(4S-6P_{3/2})} \right]^2 \left[\frac{f(4S-6P_{3/2})}{f(4S-5P_{3/2})} \right] \\ &= 30.4 \left[\frac{2070.44 \text{ cm}^{-1}}{8501.795 \text{ cm}^{-1}} \right]^2 \left[\frac{0.00296}{0.01583} \right] = 0.34 \end{aligned}$$

which agrees well with the experimental result, 0.3.

For the $4s^2S_{1/2}-np^2P_{1/2,3/2}$ ($n = 5, 6$) two-photon resonances, the peaks corresponding to the fine structures are well separated, see figure 4. For the $4s^2S_{1/2}-5p^2P_{3/2}$ and $4s^2S_{1/2}-5p^2P_{1/2}$ two-photon resonances, the ratio of SH intensities corresponding to the two resonances can be considered to be determined only by the ratio of their $\chi^{(3)}$ values because these two resonances are so close to each other that all the conditions can be assumed to be same. From table 1, we have

$$\frac{I_2(4S-5P_{3/2})}{I_2(4S-5P_{1/2})} = \frac{|\chi^{(3)}|^2_{4S-5P_{3/2}}}{|\chi^{(3)}|^2_{4S-5P_{1/2}}} = \left(\frac{16.6}{13.4} \right)^2 = 1.5.$$

When compared with the experimental value of 1.6, see figure 4, the agreement is very good. Similarly for the $4s^2S_{1/2}-6p^2P_{3/2}$ and $4s^2S_{1/2}-6p^2P_{1/2}$ two-photon resonances, we have

$$\frac{I_2(4S-6P_{3/2})}{I_2(4S-6P_{1/2})} = 3.5$$

which is large compared with the experimental value of 1.8. Here we do not consider the effect of the population reduction caused by ionisation because no enhancement in the ionisation current is observed as the laser is tuned to the $4s^2S-np^2P$ two-photon resonances, which are quite different from the $4s^2S-ns^2S$ and $4s^2S-nd^2D$ two-photon resonances, where the ionisation is strongly enhanced by the two-photon resonance (see figure 4). The $4s^2S-np^2P$ two-photon transitions are strictly forbidden in the dipole approximation. Though the generated SH radiation can make the $4s^2S-np^2P$ one-photon transition, it has no observable effect on the ionisation because this process becomes higher order.

The conversion efficiency $\eta_{SH} = I_2/I_1$ was measured on each two-photon resonance. The input energy was kept at 3 mJ during this measurement. The results are listed in table 1. For the $4s^2S-5p^2P$ and $4s^2S-6p^2P$ two-photon resonances, the conversion efficiencies are within an order of magnitude in agreement with the results of Dinev (1988b) for the $4s^2S-np^2P$ ($n = 12-21$) two-photon resonances.

3.2. SHG as laser detuning from the two-photon resonances

The SH intensities and corresponding ionisation currents, as a function of the laser detuning from the two-photon resonance, were measured, as shown in figure 4. A 'three dimensional' diagram of SH spectra for laser scanning near the $4s^2S-5p^2P$ two-photon resonance is shown in figure 5. The wavelengths corresponding to the peak values of SHG are in agreement with the energy level data from Bashkin and Stoner (1975) within this experimental accuracy. No shift has been observed. It is interesting to notice that the SHG can appear continuously when the laser wavelength is scanned from the $4s^2S-4d^2D$ to the $4s^2S^2S-6s^2S$ two-photon resonance. From the

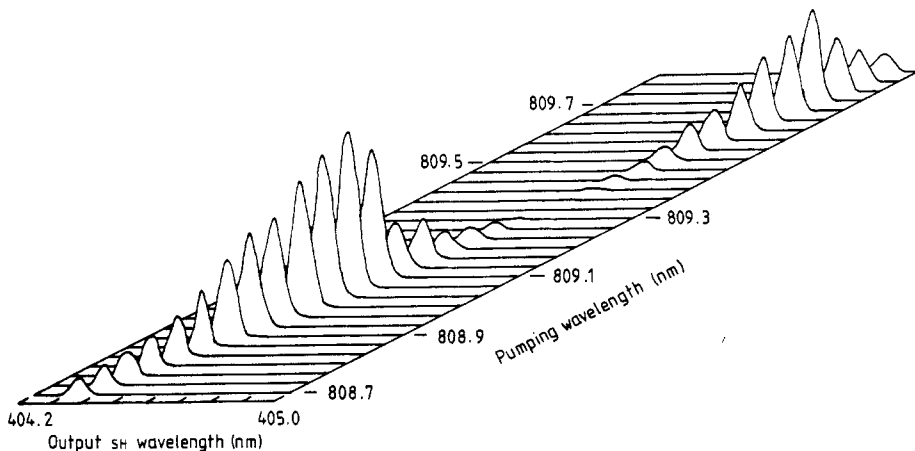


Figure 5. A 'three-dimensional' diagram of SH spectra as the laser wavelength scans near the $4s^2S-5p^2P$ two-photon resonances.

SH spectra in figure 4, we find that there exists a shoulder at one side of each resonance peak. These shoulders are considered to be due to the phase matching, which becomes very important as the laser is detuned from the resonances and makes the SH spectra asymmetric to the resonant peaks.

3.3. Intensity and density dependence of SHG

The intensity dependence of SHG on or near the two-photon resonances was measured for the laser intensity in the range 2×10^7 – 3×10^8 W cm⁻². Some typical log-log dependence curves are shown in figure 6(a–c). A slope of 2 is found when the laser is detuned from the $4s^2S$ – $ns^2S(d^2D)$ two-photon resonances. The intensity-dependence curves for the laser detuning $\Delta\nu = -5.56$ cm⁻¹ from the $4s^2S_{1/2}$ – $6s^2S_{1/2}$ two-photon resonance and $\Delta\nu = -2.1$ cm⁻¹ from the $4s^2S_{1/2}$ – $3d^2D_{5/2}$ two-photon resonance are shown in figure 6(a, c). However, a slope of 1 is found when the laser is detuned $\Delta\nu = -2.1$ cm⁻¹ from the $4s^2S_{1/2}$ – $6p^2P_{1/2}$ two-photon resonances, as shown in figure 6(b). From figure 6(c), we also notice that near the $4s^2S_{1/2}$ – $3d^2D_{5/2}$ two-photon resonance ($\Delta\nu = -2.1$ cm⁻¹) a variation of slope from 6 to 2 is found as the input intensity increases. However, as the laser is tuned to the $4s^2S$ – $6s^2S$, $4s^2S$ – np^2P ($n = 5, 6$), and $4s^2S$ – nd^2D ($n = 3, 4$) two-photon resonances, a slope of $\sim \frac{1}{2}$ is found, which is quite different from values given in previously published papers, where a slope of 2 was reported. The measured intensity-dependence curves on the $4s^2S_{1/2}$ – $6s^2S_{1/2}$, $4s^2S_{1/2}$ – $6p^2P_{3/2}$ and $4s^2S_{1/2}$ – $3d^2D_{5/2}$ two-photon resonances are shown in figure 6(a–c).

Filtering is necessary because there is a high level of background radiation from the laser and other parametric emissions, which usually are so strong and close to the SH in wavelength that it is difficult to measure the SHG on the $4s^2S$ – $ns^2S(d^2D)$ resonances without proper filtering. In this experiment two filters were used to exclude the strong background radiation almost completely, which made the accurate measurement of SHG on the $4s^2S$ – $ns^2S(d^2D)$ two-photon resonances possible. For the $4s^2S$ – np^2P two-photon resonances, the SHG measurements become very simple because no other parametric emissions close to SHG co-exist. For the same reason, it is easy to measure the SHG as laser detuning from the $4s^2S$ – $ns^2S(d^2D)$ two-photon resonances.

On the $4s^2S$ – $ns^2S(d^2D)$ two-photon resonances, the $I_1^{1/2}$ dependence of the SHG is considered to be due to saturation effects. A similar saturation effect was observed in third harmonic generation (THG) by Wang and Davis (1975) and Ward and Smith (1975). For comparison, we also measured the intensity dependence of THG on the $4s^2S_{1/2}$ – $3d^2D_{5/2}$ two-photon resonance. The results are shown in figure 6(c) and a similar saturation effect is observed. In fact, in the $\chi^{(3)}$ model, the SHG is almost the same process as the THG. Both consist completely of four-wave mixing through the third-order susceptibility $\chi^{(3)}$. It is expected that the saturation is caused by similar mechanisms in both cases. In the above papers, the saturation was attributed to the two-photon absorption of the fundamental wave or single-photon absorption of the generated wave, which reduces the population difference, and the multi-photon ionisation, which reduces the particle number in the ground state.

In this experiment, on the $4s^2S$ – $ns^2S(d^2D)$ two-photon resonances, the saturation could be caused by both the population depletion in the ground state due to the resonance-enhanced multiphoton ionisation and the reduction of population difference $\bar{N}(g \rightarrow f)$ due to the two-photon transition. On the $4s^2S$ – np^2P two-photon resonances, the saturation could be caused by both the population depletion in the ground state

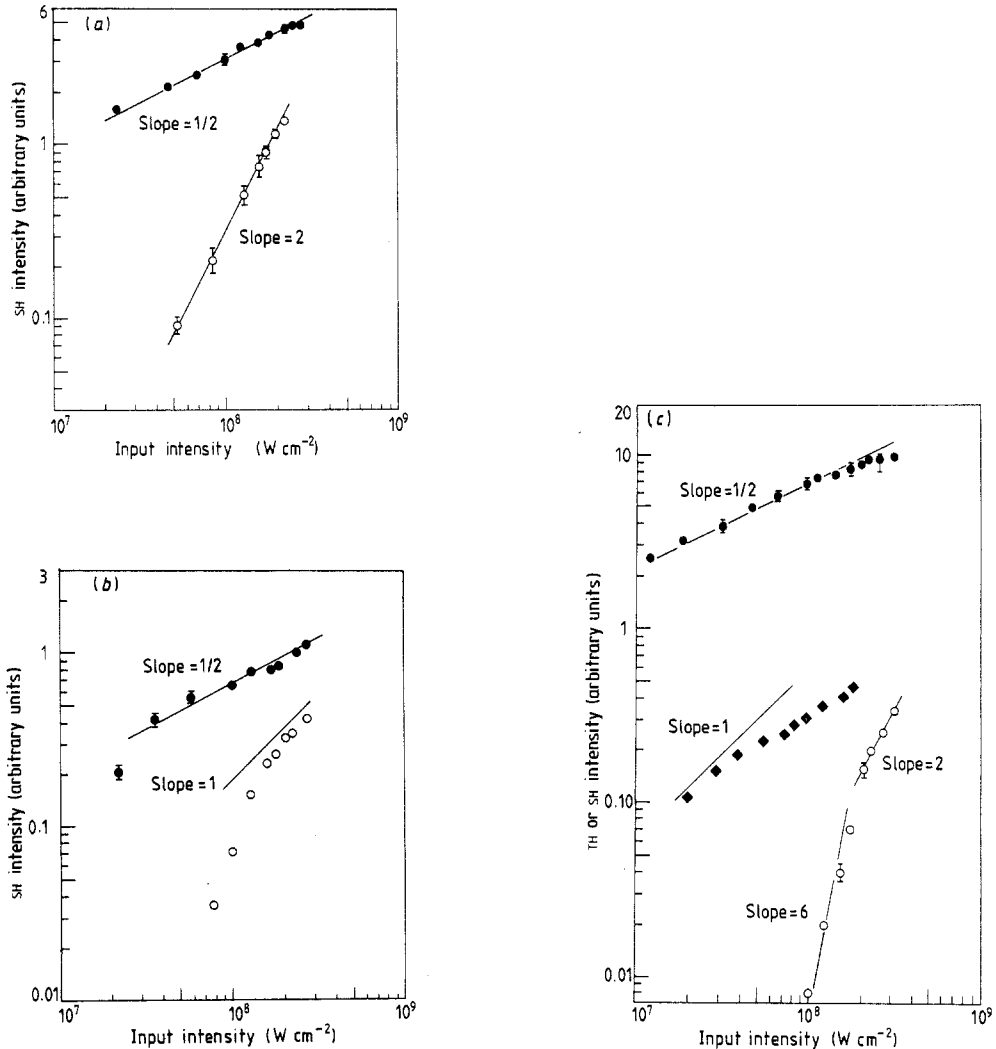


Figure 6. Intensity dependence of SHG: (a) on (●) and near (○, $\Delta\nu = -5.6 \text{ cm}^{-1}$) the $4s^2S_{1/2}-6s^2S_{1/2}$ two-photon resonance; (b) on the $4s^2S_{1/2}-6p^2P_{3/2}$ two-photon resonance (●) and near the $4s^2S_{1/2}-6p^2P_{1/2}$ two-photon resonance (○, $\Delta\nu = -2.1 \text{ cm}^{-1}$); (c) on (●) and near (○, $\Delta\nu = -2.1 \text{ cm}^{-1}$) the $4s^2S_{1/2}-3d^2D_{5/2}$ two-photon resonance—here, for comparison, the intensity dependence of THG on the $4s^2S_{1/2}-3d^2D_{5/2}$ two-photon resonance is included (◆).

due to multiphoton ionisation without resonant enhancement and the reduction of population difference due to the single-photon absorption of the generated SH. Near the $4s^2S-ns^2S(d^2D)$ two-photon resonances, the I_1^2 dependence of SHG still comes from some saturation because the intensity dependence should be I_1^3 if a laser-induced DC electric field and a three-photon ionisation are considered. In this case the ionisation is still enhanced by the near-resonances and causes the saturation of SHG to some extent. Near the $4s^2S-np^2P$ two-photon resonances, the linear intensity dependence of SHG means that single-photon absorption of the generated SH wave has much stronger effect on the SHG.

In order to understand the effect of the ionisation on the SHG, we first consider the k -photon ionisation near two-photon resonances. The particle number in the ground state at time t is given by a rate equation:

$$d N_g(t)/d t = -\sigma^{(k)} I_1^k N_g(t) \quad (7)$$

where $\sigma^{(k)}$ is the cross section for the k -photon ionisation. Here the lifetime of ions is assumed to be much longer than the laser pulse duration (20 ns). If we assume that I_1 is a constant during the pulse duration, equation (7) can be solved as

$$N_g(t) = N_0 \exp(-\sigma^{(k)} I_1^k t) \quad (8)$$

and

$$N_i(t) = N_0 [1 - \exp(-\sigma^{(k)} I_1^k t)] \quad (9)$$

where N_0 is the initial atom density and N_i is the ion density. Let us evaluate the laser induced DC field E_0 in the limit case where the time for the ionised electrons to sweep out of the laser interaction region is very short (smaller than 1 ns) as compared with the laser pulse duration 20 ns. The DC field produced by the ions in the radial direction is given by the Gauss law as:

$$E_{0r} = \frac{e}{\epsilon_0} \frac{1}{r} N_0 \int_0^r [1 - \exp(-\sigma^{(k)} I_1^k t)] r' dr'. \quad (10)$$

Here I_1 should have a Gaussian profile at the radial direction. If the escape time of electrons is not so short as we assumed, it will only change the radial profile of the induced DC field, but not influence its power dependence. For simplicity, the intensity of the laser beam is approximated by a constant, then equation (10) gives

$$E_{0r} \propto N_i = N_0 [1 - \exp(-\sigma^{(k)} I_1^k t)]$$

or

$$I_{0r} \propto N_0^2 [1 - \exp(-\sigma^{(k)} I_1^k t)]^2. \quad (11)$$

With equation (2) we have

$$\chi^{(3)} \propto \bar{N} = N_0 \exp(-\sigma^{(k)} I_1^k t). \quad (12)$$

For the $\text{sinc}(\frac{1}{2}\Delta kL)$ function in equation (1), we have

$$\begin{aligned} \text{sinc}(\frac{1}{2}\Delta kL) &= \frac{\sin(\frac{1}{2}\Delta kL)}{(\frac{1}{2}\Delta kL)} \propto \frac{\sin(\frac{1}{2}\Delta kL)}{n(2\omega) - n(\omega)} \propto \frac{\sin(\frac{1}{2}\Delta kL)}{N_g} \\ &\propto [N_0 \exp(-\sigma^{(k)} I_1^k t)]^{-1} \sin(\frac{1}{2}\Delta kL). \end{aligned} \quad (13)$$

So from equation (1), we have

$$\begin{aligned} I_2 &\propto |\chi^{(3)}|^2 I_1^2 I_0 \text{sinc}^2(\frac{1}{2}\Delta kL) \propto \frac{\bar{N}^2 I_1^2 N_i^2}{N_g^2} \sin^2(\frac{1}{2}\Delta kL) \\ &= \frac{[N_0 \exp(-\sigma^{(k)} I_1^k t)]^2 I_1^2 N_0^2 (1 - \exp(-\sigma^{(k)} I_1^k t))^2 \sin^2(\frac{1}{2}\Delta kL)}{[N_0 \exp(-\sigma^{(k)} I_1^k t)]^2} \\ &= N_0^2 I_1^2 [1 - \exp(-\sigma^{(k)} I_1^k t)]^2 \sin^2(\frac{1}{2}\Delta kL) \end{aligned} \quad (14)$$

which gives a quadratic density dependence for SHG and also a quadratic intensity dependence for SHG as $(\sigma^{(k)}I_1^k t)$ becomes large. If $(\sigma^{(k)}I_1^k t)$ is small, $[1 - \exp(-\sigma^{(k)}I_1^k t)]^2$ can be approximated by $(W^{(k)}I_1^k t)^2$ and $I_2 \propto I_1^{2k+2}$. So a slope of 10 is expected at low intensity I_1 near the $4s^2S_{1/2}-3d^2D_{5/2}$ two-photon resonance, in which the four-photon ionisation occurs. Actually, in this experiment a slope of 6 was observed at the laser intensity $\sim 10^8$ W cm $^{-2}$, as shown in figure 6(c). Here a smooth change of the factor $\text{sinc}^2(\frac{1}{2}\Delta kL)$ is assumed. As $(\sigma^{(k)}I_1^k t)$ becomes so large that all the atoms are ionised, then $\text{sinc}^2(\frac{1}{2}\Delta kL) \rightarrow 1$ because $\Delta k \propto N_g \rightarrow 0$. The SH intensity becomes

$$I_2 \propto N_0^4 I_1^2 \exp(-2\sigma^{(k)}I_1^k t) \quad (15)$$

which exponentially decays to zero.

Under the $4s^2S-ns^2S(d^2D)$ two-photon resonances, we have to consider the two-photon absorption. The rate equation for the particle number in the ground state should be written as

$$dN_g(t)/dt = -\sigma^{(k)}I_1^k N_g(t) - \sigma^{(2)}I_1^2 N_g(t) \quad (16)$$

where $\sigma^{(2)}$ is the cross section of two-photon absorption. Here the lifetimes of the excited states due to the two-photon transitions are assumed to be much longer than the laser pulse duration, so we ignore the fact that the excited states caused by the two-photon absorption return to the ground state. From equation (16), the particle number in ground state is

$$N_g(t) = N_0 \exp[-(\sigma^{(k)}I_1^k + \sigma^{(2)}I_1^2)t]. \quad (17)$$

The ion number $N_i(t)$ and the particle number in the two-photon excited state $N_f(t)$ can be expressed, respectively, by

$$N_i(t) = N_0 \frac{\sigma^{(k)}I_1^k}{\sigma^{(k)}I_1^k + \sigma^{(2)}I_1^2} \{1 - \exp[-(\sigma^{(k)}I_1^k + \sigma^{(2)}I_1^2)t]\} \quad (18)$$

and

$$N_f(t) = N_0 \frac{\sigma^{(2)}I_1^2}{\sigma^{(k)}I_1^k + \sigma^{(2)}I_1^2} \{1 - \exp[-(\sigma^{(k)}I_1^k + \sigma^{(2)}I_1^2)t]\}. \quad (19)$$

Similar to the analysis for the non-resonances, we have

$$I_0 \propto N_i^2 = N_0^2 \left(\frac{\sigma^{(k)}I_1^k}{\sigma^{(k)}I_1^k + \sigma^{(2)}I_1^2} \right)^2 \{1 - \exp[-(\sigma^{(k)}I_1^k + \sigma^{(2)}I_1^2)t]\}^2 \quad (20)$$

$$\chi^{(3)} \propto \bar{N} = N_g(t) - N_f(t)$$

$$\begin{aligned} &= N_0 \left(\frac{\sigma^{(k)}I_1^k + 2\sigma^{(2)}I_1^2}{\sigma^{(k)}I_1^k + \sigma^{(2)}I_1^2} \exp[-(\sigma^{(k)}I_1^k + \sigma^{(2)}I_1^2)t] \right. \\ &\quad \left. - \frac{\sigma^{(2)}I_1^2}{\sigma^{(k)}I_1^k + \sigma^{(2)}I_1^2} \right) \quad (21) \end{aligned}$$

and

$$\text{sinc}(\frac{1}{2}\Delta kL) \propto \sin(\frac{1}{2}\Delta kL) / N_g = [N_0 \exp[-(\sigma^{(k)}I_1^k + \sigma^{(2)}I_1^2)t]]^{-1} \sin(\frac{1}{2}\Delta kL). \quad (22)$$

So the SH intensity becomes

$$\begin{aligned}
 I_2 &\propto |\chi^{(3)}|^2 I_1^2 I_0^2 \text{sinc}^2(\frac{1}{2}\Delta kL) \\
 &\propto N_0^2 I_1^2 \left(\frac{\sigma^{(k)} I_1^k}{\sigma^{(k)} I_1^k + \sigma^{(2)} I_1^2} \right)^2 \{1 - \exp[-(\sigma^{(k)} I_1^k + \sigma^{(2)} I_1^2)t]\}^2 \\
 &\quad \times \left(\frac{\sigma^{(k)} I_1^k + 2\sigma^{(2)} I_1^2}{\sigma^{(k)} I_1^k + \sigma^{(2)} I_1^2} - \frac{\sigma^{(2)} I_1^2}{\sigma^{(k)} I_1^k + \sigma^{(2)} I_1^2} \exp[(\sigma^{(k)} I_1^k + \sigma^{(2)} I_1^2)t] \right)^2 \\
 &\quad \times \text{sinc}^2(\frac{1}{2}\Delta kL). \tag{23}
 \end{aligned}$$

When $(\sigma^{(k)} I_1^k + \sigma^{(2)} I_1^2)t$ is small, the term in the last set of two line parentheses can be approximated by

$$\frac{\sigma^{(k)} I_1^k + 2\sigma^{(2)} I_1^2}{\sigma^{(k)} I_1^k + \sigma^{(2)} I_1^2} - \frac{\sigma^{(2)} I_1^2}{\sigma^{(k)} I_1^k + \sigma^{(2)} I_1^2} \exp[(\sigma^{(k)} I_1^k + \sigma^{(2)} I_1^2)t] \sim \frac{1}{1 + \sigma^{(2)} I_1^2 t}.$$

Then I_2 becomes

$$\begin{aligned}
 I_2 &\propto N_0^2 \left(\frac{I_1}{1 + \sigma^{(2)} I_1^2 t} \right)^2 \left(\frac{\sigma^{(k)} I_1^k}{\sigma^{(k)} I_1^k + \sigma^{(2)} I_1^2} \right)^2 \\
 &\quad \times \{1 - \exp[-(\sigma^{(k)} I_1^k + \sigma^{(2)} I_1^2)t]\}^2 \text{sinc}^2(\frac{1}{2}\Delta kL) \tag{24}
 \end{aligned}$$

which reflects the saturation effect. That is why the $I_1^{1/2}$ dependence of SHG was observed on the $4s^2S$ - ns^2S (d^2D) two-photon resonances. In general, the cross section of two-photon absorption is many orders of magnitude larger than that of multiphoton ionisation. However, the ionisation cross section on the two-photon resonances could be enhanced by many orders of magnitude. At high laser intensity the $\sigma^{(k)} I_1^k$ can be larger than $\sigma^{(2)} I_1^2$. So the saturation effect is more obvious and stronger on the $4s^2S$ - ns^2S (d^2D) two-photon resonances. When the laser intensity becomes so large that all particles are excited or ionised, the $\text{sinc}(\frac{1}{2}\Delta kL)$ approaches 1 because $\Delta k \propto N_g \rightarrow 0$ and the SH intensity becomes

$$I_2 \propto N_0^4 I_1^2 \exp(-2\sigma^{(k)} I_1^k t) \tag{25}$$

which will decay exponentially to zero.

On the $4s^2S$ - np^2P two-photon resonances no enhancement of ionisation has been observed, see figure 4. Therefore, in these cases the ion density should be the same as that for the non-resonances, given by equation (9),

$$N_i(t) = N_0[1 - \exp(-\sigma^{(k)} I_1^k t)]. \tag{26}$$

Considering the single-photon absorption, the rate equation for the particle number in the ground state on the $4s^2S$ - np^2P two-photon resonances should be

$$dN_g(t)/dt = -\sigma^{(k)} I_1^k N_g(t) - \sigma^{(1)} I_2 N_g(t). \tag{27}$$

So we have

$$N_g(t) = N_0 \exp[-(\sigma^{(k)} I_1^k + \sigma^{(1)} I_2)t]. \tag{28}$$

The particle number in the one-photon excited state (the np^2P state) is given by

$$N_f(t) = N_0 - N_i - N_g = N_0[1 - \exp(-\sigma^{(1)} I_2 t)] \exp(-\sigma^{(k)} I_1^k t). \tag{29}$$

With the same procedure as we use for the $4s^2S$ - ns^2S (nd^2D) two-photon resonances we have

$$I_2 \propto N_0^2 I_1^2 [2 - \exp(\sigma^{(1)} I_2 t)]^2 [1 - \exp(-\sigma^{(k)} I_1^k t)]^2 \text{sinc}^2(\frac{1}{2}\Delta kL). \tag{30}$$

As $(\sigma^{(1)}I_2t)$ is small ($\ll 1$), the factor $[2 - \exp(\sigma^{(1)}I_2t)]^2$ can be expanded in series. If we take only the first-order term in the series, equation (30) becomes

$$I_2 = AN_0^2I_1^2[1 - 2\sigma^{(1)}I_2t][1 - \exp(-\sigma^{(k)}I_1^k t)]^2 \sin^2(\frac{1}{2}\Delta kL) \quad (31)$$

where A is a constant. Then I_2 can be solved as

$$I_2 = \frac{AN_0^2I_1^2[1 - \exp(-\sigma^{(k)}I_1^k t)]^2 \sin^2(\frac{1}{2}\Delta kL)}{1 + 2AN_0^2\sigma^{(1)}tI_1^2[1 - \exp(-\sigma^{(k)}I_1^k t)]^2 \sin^2(\frac{1}{2}\Delta kL)} \quad (32)$$

which gives the saturation when the second term in the denominator becomes larger. Since the single-photon absorption cross section is usually many orders of magnitude larger than the two-photon absorption cross section, it is expected that the saturation effect for the $4s^2S-np^2P$ two-photon resonances is much more obvious even though the laser is detuned from the two-photon resonances, where linear intensity dependence is observed, in contrast with the detuning from the $4s^2S-ns^2S(d^2D)$ two-photon resonances where quadratic dependence is observed.

The density dependence of SHG on the $4s^2S_{1/2}-6s^2S_{1/2}$ and $4s^2S-5p^2P_{3/2}$ two-photon resonances and near the $4s^2S_{1/2}-6s^2S_{1/2}$ two-photon resonance ($\Delta\nu = -5.65 \text{ cm}^{-1}$) were measured, as shown in figure 7. A quadratic dependence is observed, as given by equations (14) and (24). It is interesting to notice that for the $4s^2S_{1/2}-5p^2P_{3/2}$ two-photon resonance, the density-independence of SHG has been observed at high density (shown in figure 7). This result can be exactly predicted by equation (32), in which I_2 becomes independent of the density N_0 as N_0 increases.

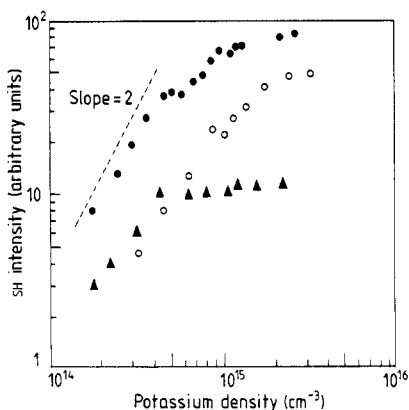


Figure 7. Vapour density dependence of SHG on (●) and near (○, $\Delta\nu = -5.6 \text{ cm}^{-1}$) the 4S-6S two-photon resonance and on the 4S-5P_{3/2} two-photon resonance (▲). Here the laser intensity is $I_1 = 1.7 \times 10^8 \text{ W cm}^{-2}$.

4. Conclusion

We have measured the SH spectra and the corresponding ionisation currents on or near the $4s^2S-6s^2S$, $4s^2S-np^2P$ ($n = 5, 6$), and $4s^2S-nd^2D$ ($n = 3, 4$) two-photon resonances in potassium vapour. Some ratios of the SH intensities related to different

two-photon resonances have been calculated using the $\chi^{(3)}$ model and comparisons with the measurements have been made. The intensity and density dependence of SHG has also been analysed with this model. The results show that most of the characteristics of SHG in our experiment can be explained using the $\chi^{(3)}$ model, i.e. the four-wave mixing which includes a laser-induced DC electric field.

The multiphoton ionisation, on the one hand, produces the DC electric field, which is necessary for SHG in the $\chi^{(3)}$ model. On the other hand, the ionisation causes the population depletion of the ground state, which reduces the SHG. For the $4s^2S-ns^2S(d^2D)$ two-photon resonances, the multiphoton ionisation enhanced by the two-photon resonances and the two-photon transition are responsible to the saturation in the intensity dependence of SHG. However, for the $4s^2S-np^2P$ two-photon resonances, the multiphoton ionisation without any observable resonant enhancement and the single-photon absorption of the generated SH wave are responsible to the saturation effects. The saturation in SHG is much like that in THG, which is a typical parametric process—four-wave mixing. So the similarity between the SHG and THG seems to indicate the same mechanism for both processes.

In the collision model for SHG (Elci and Depatie 1988) a collision complex composed of two atoms is assumed to exist. The energy levels of the complex should have some shifts to those of the free atoms. We notice that in this case, where only low-lying excited states are involved, the p states and the s (or d) states are separated by so far that the l mixing by collision is almost impossible without a remarkable energy shift. These shifts should be observed when the SH wavelengths corresponding to the two-photon resonances are measured. No shifts have been observed in this experiment.

Acknowledgment

This project was supported by the National Science Council of the Republic of China.

References

- Bashkin S and Stoner J O 1975 *Atomic Energy Levels and Grotrian Diagrams* (Amsterdam: North-Holland)
- Bethune D S 1981 *Phys. Rev. A* **23** 3139
- Dinev S G 1988a *J. Phys. B: At. Mol. Opt. Phys.* **21** 1681
- 1988b *Opt. Quantum Electron.* **20** 113
- Dinev S G, Guzman de Carcia A, Meystre P, Salomaa R and Walther H 1983 *Laser Spectroscopy VI* ed H P Weber and W Luthy (Berlin: Springer) p 183
- Eicher H 1975 *IEEE J. Quantum Electron* **QE-11** 121
- Elci A and Depatie D 1988 *Phys. Rev. Lett.* **60** 688
- Gallagher T F, Edelstein S A and Hill R M 1977 *Phys. Rev. A* **15** 1945
- Hanna DC, Yuratich M A and Kotter D 1979 *Nonlinear Optics of Free Atoms and Molecules* (Berlin: Springer)
- Lindgard A and Nielsen S E 1977 *At. Data Nucl. Data Tables* **19**
- Lu M H and Tsai J H 1989 *Chinese J. Phys.* **27** 14
- Mossberg T, Flusberg A and Hartmann S P 1978 *Opt. Commun.* **25** 121
- Okada J, Fukuda Y and Matsuoka M 1981 *J. Phys. Soc. Japan* **50** 1301
- Vidal C R and Cooper J 1969 *J. Appl. Phys.* **40** 3370
- Wang C C and Davis L I Jr 1975 *Phys. Rev. Lett.* **35** 650
- Ward J F and Smith A V 1975 *Phys. Rev. Lett.* **35** 653